Salt and Specific Cation Effects in the Quenching of Triplet State Tetrakis(*μ*-pyrophosphite-*P,P′*)diplatinate(II) by Acidopentacyanocobaltate(III) Anions

Le-Zhen Cai,[§] Diane M. Kneeland,[‡] and Alexander D. Kirk*[,†]

Department of Chemistry, University of Victoria P.O. Box 3065, Victoria, BC, Canada V8W 3V6, and Department of Chemistry, University of Texas Austin, Texas 78712

Received: October 30, 1996; In Final Form: March 4, 1997[⊗]

In the presence of moderate to high concentrations of electrolytes, the emission of $*[Pt_2(pop)_4]^{4-}$ (where pop = *μ*-pyrophosphite-*P,P′*) is quenched by the complexes $[Co(CN)_5X]^{3-}$ (where X = N_3^-, I^-, Br^-, Cl^-, but not CN^-). The salt effects on the emission decay lifetime quenching rate constants between these anionic species have been studied in the presence of MCl, M′Cl_2, or $R_nNH_{4-n}Cl$ (where M, M′, and R represent alkali, alkaline earth metals, and alkyl respectively, $n = 0-3$) and K_nX (X = Cl^-, Br^-, NO_3^-, SO_4^{2-}, $[Co(CN)_6]^{3-}$, $n = 1-3$). At 0.5 M cation concentration, second-order quenching rate constants, k_q, are in the "nearly diffusion-controlled" range, 10^7-10^9 L mol^{-1} s^{-1}, and k_q decreases by an order of magnitude across the series of quenchers $[Co(CN)_5I]^{3-} > [Co(CN)_5N_3]^{3-} > [Co(CN)_5Br]^{3-} > [Co(CN)_5Cl]^{3-}$. On the basis of a detailed study of $[Co(CN)_5I]^{3-}$, the quenching efficiency increases with background electrolyte concentration and the measured rate constants are in good agreement with predictions based on the Debye−Smoluchowski and Debye−Eigen equations for diffusion-controlled formation and dissociation in ionic solution of an encounter pair, together with a rate constant of 1.2×10^9 s^{-1} for the quenching step. However, the analysis provides further evidence for the Olson−Simonson effect; that is, in the presence of multivalent electrolyte ions, the salt effects are determined by the counterion concentration, here the cation, rather than by the ionic strength. Specific cation effects are observed such that the quenching rate constants increase in the following sequences: $Li^+ < Na^+ < K^+ < Cs^+$; $Mg^{2+} < Ca^{2+} < Sr^{2+} < Ba^{2+}$; $NH_4^+ < MeNH_3^+ < Me_2NH_2^+ < Me_3NH^+$; $Et_3NH^+ < Et_2NH_2^+ < EtNH_3^+$; n-$PrNH_3^+ < EtNH_3^+ < MeNH_3^+$. For the alkali or alkaline-earth cations the large effects seen require participation of the cation in the transition state for the quenching step; the alkylammonium cations are also effective in this role, but the small differences in their efficiencies can be rationalized in terms of their effects on water structure.

Introduction

There has been a continuing interest in the study of the influence of added electrolytes on reactions between ions of the same and opposite charges. Most often these have involved ground electronic states, but the effects seem to apply equally well to reactions involving excited state species in the few examples that have been studied. As an example, the recent detailed studies[1] by Chiorboli et al. have clearly set out the factors that can be of importance. They concluded that for their system, which involved the quenching of excited state $[Ru(bpy)_3]^{2+}$ by other cations, the Debye−Smoluchowski and Debye−Eigen equations give valid predictions of diffusional rate constants up to high electrolyte concentrations. However, they found that the important variable was not the ionic strength as is usually assumed, but the concentration of the main counterion; this is the Olson−Simonson effect.[2] The Olson−Simonson effect has been previously noticed in thermal reactions between reactants of like charge such as $[Co(sep)]^{3+}$ and $Cr(H_2O)_6]^{2+}$,[3] $[Mo(CN)_8]^{3-}$ and I^-,[4] $S_2O_8^{2-}$ and $[Fe(CN)_6]^{4-}$,[5,6] $C_2H_5CO_2CO_2^-$ and OH^-,[7] $C_2H_5CO_2CH_2CO_2^-$ and OH^-,[8] and $[Fe(CN)_6]^{4-}$ and $[Fe(CN)_6]^{3-}$,[9] in $S_4O_6^{2-}$ disproportionation to give $S_3O_6^{2-}$ and $S_5O_6^{2-}$,[10] and also in the quenching of excited state $*[Ru(bpy)_3]^{2+}$ by $[Co(sep)]^{3+}$.[11]

Chiorboli et al. also reported[1] some specific ion effects, but the data on those was limited by the difficulty of finding a variety of anions that can be used without problems caused by insolubility, acid/base equilibria, or redox processes. Some examples of specific anion effects on redox reactions between cationic coordination complexes are $[FeL_3]^{3+}$ and $[OsL_3]^{2+}$ (L = bpy and its derivatives),[12] $[FeL_3]^{3+}$ and $[OsL_3]^{2+}$ (L = 4,4-dimethyl-2,2′-bipyridyl),[13] and $[Co(NH_3)_6]^{3+}$ and $[Co(NH_3)_6]^{2+}$.[14] In other studies, specific cation effects with rate constant trends such as $Li^+ < Na^+ < K^+ < Cs^+$ for alkali metals and $Mg^{2+} < Ca^{2+} < Sr^{2+} < Ba^{2+}$ for alkaline-earths, have been reported for a number of thermal electron transfer reactions occurring between anionic complexes: $[Fe(CN)_6]^{3-}$ and $[Fe(CN)]_6^{4-}$,[15] MnO_4^{2-} and MnO_4^-,[16] $[Co^{II}O_4W_{12}O_{36}]^{6-}$ and $[Co^{III}O_4W_{12}O_{36}]^{5-}$,[17] and $[W(CN)_8]^{3-}$ and As^{III}.[18] Only a few examples have been reported for specific ion effects involving the quenching reactions of excited state complexes. These are $*[Ru(bpy)_3]^{2+}$ and $[Co(sep)]^{3+}$,[11] $*[Ru(bpy)_3]^{2+}$ and methyl viologen,[1,19,20] $*[(Mo_6Cl_8)Cl_6]^{2-}$ and $[IrCl_6]^{2-}$,[21] and $*[Pt_2(pop)_4]^{4-}$ and $[Mo(CN)_8]^{4-}$.[22]

In the course of earlier work from this laboratory, we observed[23,24] specific cation effects on the ratio of photoaquation to photoanation by thiocyanate in some acidopentacyanocobaltate(III) complexes. Our ability to study these, and the general salt effects, was severely restricted by the precision of the product analysis. We therefore sought a superior experimental system in which to clarify the salt and specific cation effects associated with the interaction of these anionic complexes. We have found that they act as efficient quenchers of the triplet excited state of $[Pt_2(pop)_4]^{4-}$, as does the analogous $[Mo(CN)_8]^{4-}$ complex.[22] This has enabled us to undertake an extensive study of salt effects in this quenching process using a series of

* To whom correspondence should be addressed.
† University of Victoria.
‡ University of Texas.
§ Department of Chemistry, Concordia University, Montreal, Quebec, Canada 3HG 1M8.
⊗ Abstract published in *Advance ACS Abstracts,* April 15, 1997.

S1089-5639(96)03383-X CCC: $14.00

TABLE 1: Electronic Absorption Spectra Data λ_{max}, nm (ϵ) of $[Co(CN)_5X]^{3-}$ Complexes in Aqueous Solution at Room Temperature

X	this work	ref 33	ref 24	ref 30
N_3	220_{sh} (1.23×10^4)		220_{sh} (1.08×10^4)	
	281 (9.48×10^3)		280 (8.36×10^3)	
	382 (824)		380 (749)	380 (600)
I	223_{sh} (8.27×10^3)			
	262 (1.79×10^4)	260 (1.75×10^4)		
	331 (2.85×10^3)	330 (2.95×10^3)	334 (2.93×10^3)	
	408_{sh} (267)	$\sim 440_{sh}$ ($\sim$200)	408 (255)	440_{sh} (200)
	500 (93)	500 (95)	500 (107)	
Br	242 (1.71×10^4)	242 (1.32×10^4)		
	290_{sh} (1.02×10^3)	295 (822)		
	397 (190)	395 (170)	398 (172)	398 (177)
Cl	210 (1.83×10^4)	224 (1.61×10^4)		
	384 (215)	392 (200)	390 (201)	390 (200)

acidopentacyanocobalt(III)ates. We will describe separately[25,26] the reactive quenching which is found in these systems, while here we report the study of the salt and specific cation effects using a large range of electrolytes, comparing the results to theory.

Experimental Section

Preparation and Characterization of Compounds. *Potassium Acidopentacyanocobaltates, $K_3[Co(CN)_5X]$ (X = N3, I, Br, Cl).* Literature methods were used for the synthesis of the precursors $[Co(NH_3)_5N_3]Cl_2$[27] and $K_3[Co(CN)_5N_3]\cdot 2H_2O$.[28] The latter complex was carefully recrystallized to remove potassium chloride.[29] Flor and Casabo's method was used for the syntheses of the acidopentacyanocobaltate complexes,[30] but further purification was needed, especially for the chloro complex. The crude product was dissolved in the *minimum* amount of water (for the bromo and iodo complexes) or 50% ethanol (for the chloro complex) and filtered. The filtrate formed an oil when mixed with cold ethanol (0 °C), and the purest products were obtained via these oils, rather than via the solids obtained when larger initial water quantities were used. The oily product was vigorously stirred to break it into small droplets and the supernatant discarded. This cold ethanol washing was repeated until the oil solidified. The final precipitate was then filtered off, washed with cold ethanol, acetone, and ether, and vacuum dried in a desiccator. For the chloro complex only, the above purification procedure was inefficient, resulting in a low product yield.

Elemental analysis was not applicable since these compounds form refractory nitrides and carbides leading to irreproducible analytical results.[30−32] The identity and purity of the complexes were therefore established by reversed-phase HPLC (a single peak with an appropriate, different retention time was seen for each), UV−vis spectra, and X-ray powder diffraction. A comparison of our electronic absorption results with literature data, Table 1, confirms the identity of the compounds, and our somewhat higher molar absorptivity values are consistent with the high purity suggested by the chromatographic results. The strong charge transfer absorptions ($\epsilon \geq 10^3$ L mol^{-1} cm^{-1}) in the near UV and the weaker long wavelength spin-allowed d−d transitions, $^1A_1 \rightarrow {}^1E$, of the complexes have been previously assigned.[33−35] Each complex had an X-ray powder line pattern similar to potassium hexacyanocobaltate(III), but with different line spacings, and the samples were free of potassium halide, which is the likely impurity and highly distinguishable if present.

Potassium Tetrakis(μ-pyrophosphite-P,P′)diplatinate(II) Dihydrate, $K_4[Pt_2(\mu\text{-}P_2O_5H_2)_4]\cdot 2H_2O$. This complex was prepared by modifying a literature procedure.[36] A stirred solution of 0.8 g of K_2PtCl_4 and 3.0 g of H_3PO_3 (fresh 97% material stored under nitrogen) in 4−5 mL of H_2O was heated under nitrogen for about 3 h in a 100 °C glycerol bath with occasional replenishment of the water content. During the heating process, the color of the solution gradually changed from red to brown, then to yellow-green. Since drying in an oven led to a low product yield, the solution was left in the 100 °C bath and dried by N_2 flow. The solid that remained was washed with methanol and acetone to remove unreacted H_3PO_3. Purification was by dissolving in a minimum amount of degassed water, filtering (medium porosity filter (10 to 20 μm) plus a 0.45 μm Micron Sep membrane filter), and reprecipitation by degassed methanol followed quickly by acetone. Fine yellow powder formed, and the degassed, sealed system was cooled in a refrigerator overnight. The resulting yellow-green solid was filtered off under N_2, washed with methanol, acetone, and ether, and vacuum dried, yield 45%. The dry sample was air stable. Solutions in degassed water were stable for several hours, but aerated solutions turned purple or even black within an hour.

The electronic absorption spectrum of $[Pt_2(pop)_4]^{4-}$ in aqueous solution had λ_{max}, nm (ϵ): 245 (3.1×10^3), 271 (1.5×10^3), 304_{sh} (1.0×10^3), 368 (3.4×10^4), 453 (1.15×10^2), in good agreement with literature data of 244, 270 (1.4×10^3), 303 (8.5×10^2), 368 (3.5×10^4), 452 (1.2×10^2).[37] These absorption bands have been assigned as the $5d \rightarrow 6p_z$ transitions (244 and 271 nm), $d \rightarrow d$ transition (303 nm), fully allowed $^1A_{1g} \rightarrow {}^1A_{2u}$ transition (368 nm), and spin-forbidden $^1A_{1g} \rightarrow {}^3A_{2u}$ transition (450 nm).[38−40] Excitation of a room temperature aqueous solution at 330, 370, or 452 nm resulted in an intense green emission at 514 nm, which originates from the $^3A_{2u}$ excited state,[39,41] and is rather long-lived (lifetime $\tau \geq 9$ μs in aqueous solution at 22.0 °C). ^{31}P NMR: δ 68.9 ppm, $^1J(^{31}P-{}^{195}Pt) = 3076$ Hz. The ^{195}Pt NMR of the prepared compound confirmed this value of the $^{31}P-{}^{195}Pt$ coupling constant.

General Physical and Analytical Measurements. The pH of solutions was determined within ±0.01 pH units with a Fischer "Accumet" 910 digital pH meter and Ingold LOT electrode calibrated with appropriate buffers.

UV/vis spectra were run on a Phillips PU 8740 UV/Vis, Cary 5, or Cary 1 UV-Vis-NIR Spectrophotometer using 1 cm silica cells. All solutions were filtered through 0.20 μm Micro Sep membrane filters to minimize scattering.

Emission and excitation spectra were obtained from an Aminco SPF 125 double monochromator spectrofluorometer, using a 1 cm silica fluorescence cell. The light source was a xenon lamp.

^{1}H NMR, ^{13}C NMR, ^{31}P NMR, and ^{195}Pt NMR were run on a Bruker AMX 360 MHz NMR spectrometer or a Bruker B-ACS60 300 MHz NMR spectrometer. The chemical shifts (δ ppm) were reported relative to tetramethylsilane (TMS) for ^{1}H NMR and ^{13}C NMR and 85% H_3PO_4 for ^{31}P NMR.

The X-ray powder diffraction photographs of the $K_3[Co(CN)_5X]$ complexes (X = CN, Cl, Br, N_3, I) were taken using a Guinier camera with Cu Kα line ($\lambda = 1.542$ Å) radiation.

For analysis of the complexes $[Co(CN)_5X]^{3-}$ (X = CN, Cl, Br, N_3, I) by ion pair reversed-phase HPLC, a Varian 5000 liquid chromatograph with a variable wavelength UV−vis detector was used in conjunction with a 25 × 0.46 cm Chromatographic Sciences ODS2 10 μm C_{18} column. Two eluents were made up containing 25 mM *n*-octylammonium as ion interaction reagent and 25 mM sodium citrate as modifier using water, A, and 50% v/v aqueous methanol, B, as solvents. The pH of these eluents was adjusted to 6.5 to ensure that the citrate was present in the 3− form. It was found that an isocratic combination of the eluents with 80% B, flowing at 2 mL min^{-1}, gave the best separations. The detection wavelength was 240 nm.

Emission Decay Lifetime Measurements. A PTI PL 2300 Nitrogen Laser of pulse energy 1.5 mJ at 337 nm, filtered through a Corning CS 7-54 filter, was used at 3 Hz. As fill gas, 99.999% nitrogen was further purified by hydrocarbon and 13 X molecular sieve Moisture Traps (Chromatographic Specialties Inc.). At 337 nm $[Pt_2(pop)_4]^{4-}$ has a much smaller molar absorptivity than the cobalt quenchers $[Co(CN)_5X]^{3-}$ so that use of this wavelength at appropriate quencher and $[Pt_2(pop)_4]^{4-}$ concentrations would have led to enormous inner filter effects in the Stern−Volmer studies. Quinine sulfate in ethanol was therefore used as a wavelength shifter. It has a strong absorption between 320 and 340 nm ($\log \epsilon = 4$) and emits with a short fluorescence lifetime,[42] 19.2 ns, at 370 nm, where $\epsilon([Pt_2(pop)_4]^{4-}) \gg \epsilon([Co(CN)_5I]^{3-})$. The laser beam was intercepted in a 1 cm rectangular cell containing quinine solution in contact with the sample cell. The absorbance of the ethanolic quinine sulfate solution at 337 nm was adjusted to 3.0 (ca. 3×10^{-4} M), and fresh solution was used for each quenching experiment. Both cells were held in a thermostated cell compartment maintained at 22.0 ± 0.1 °C. Presaturated nitrogen was bubbled into the working solution for degassing and mixing after the addition of quencher. The $[Pt_2(pop)_4]^{4-}$ emission was filtered by a Corning CS 3-72 glass filter, a $K_2Cr_2O_7$ solution filter to remove wavelengths shorter than 500 nm, and a neutral density filter to avoid overloading the photomultiplier. The emission decay was detected at right angles to the laser beam by a Jarrel-Ash 82-410 monochromator set at 514 nm/Hamamatsu R928 GaAs photomultiplier/Tektronix 2230 digital storage oscilloscope detector system (connected with 200 Ω load resistor) with a GPIB interface to an ATARI 1040 microcomputer. Lifetimes were evaluated by weighted linear regression on a plot of ln(intensity) versus time[43] over 1024 channels of decay.

Kinetic Data and Salt and Cation Effects. Solutions of MCl (M = Li^+, Na^+, K^+, Cs^+), M′Cl_2 (M′ = Mg^{2+}, Ca^{2+}, Sr^{2+}, Ba^{2+}), $R_nNH_{4-n}Cl$ (R = H, Me, Et, *n*-Pr, $n = 0-3$), or K_nX (X = Br^-, NO_3^-, SO_4^{2-}, $[Co(CN)_6]^{3-}$, $n = 1-3$) electrolytes (usually 0.500 M in cation concentration) were prepared in 0.010 M $HClO_4$ aqueous solution. The solutions were kept in polyethylene bottles to avoid leaching of quenching impurities[24] from glass containers. $[Pt_2(pop)_4]^{4-}$ solution was freshly prepared in the appropriate electrolyte to give an absorbance of about 1 in a 1 cm path at 370 nm (about 2×10^{-5} M). The solution was then purged with nitrogen until the lifetime reached a constant upper limit, τ°. The quencher, also dissolved in the appropriate electrolyte, was delivered into the $[Pt_2(pop)_4]^{4-}$ solution in 7−12 aliquots, 5−20 μL in volume, and each lifetime was determined at least five times. The $[Pt_2(pop)_4]^{4-}$ lifetime was reduced by about half overall, at which point, even for the strongly absorbing iodo and azido complexes, the fraction of light absorption by quencher was less than 50%. The quenching rate constant k_q was obtained from the slope of a Stern−Volmer plot of τ°/τ versus quencher concentration, and each quenching experiment was repeated 2−5 times.

Results

Quenching Rate Constants. In a thoroughly deaerated aqueous solution with no quencher, $[Pt_2(pop)_4]^{4-}$ showed an emission decay lifetime of 9.7 μs, in good agreement with the literature[38,44,45] value. The lifetime was shortened to 8−9 μs in acidic media, but on addition of Cl^-, no change was observed within the experimental error of ±0.1 μs. No self-quenching of phosphorescence was observed under our experimental conditions, where $[Pt_2(pop)_4]^{4-}] \approx 3 \times 10^{-5}$ M, and this is consistent with the report by Kalyanasundaram[46] that it occurs only at $[Pt_2(pop)_4]^{4-}$ concentrations greater than 10^{-4} M. Buffer solutions were not used because of the reported[47] decomposition of $[Pt_2(pop)_4]^{4-}$ in pH 7 buffer. Instead, the quenching study was performed in a 0.010 M $HClO_4$ medium to ensure that more than 90% of $[Pt_2(pop)_4]^{4-}$ existed as the 4− anion ($pK_{a1} = 3.0$, $pK_{a2} = 8.0$[44]). It was found that no $[Pt_2(pop)_4]^{4-}$ quenching occurred with any of the cobalt complexes in the absence of added electrolyte.

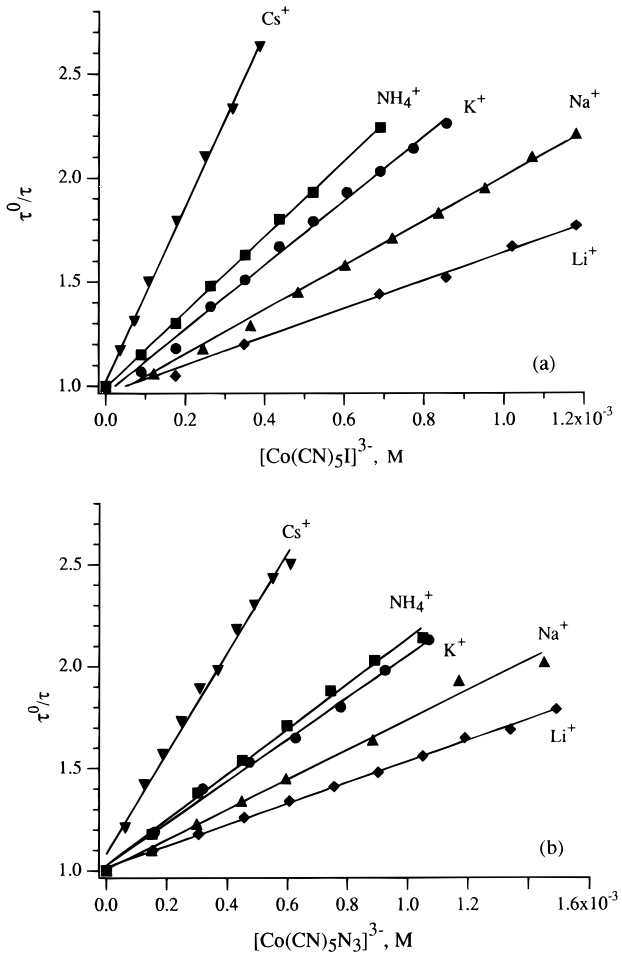

Figure 1. Stern−Volmer plots for quenching of *$[Pt_2(pop)_4]^{4-}$ by $[Co(CN)_5X]^{3-}$ in 0.50 M MCl/0.010 M $HClO_4$ solution. (a) X = I; (b) $X = N_3$. Markers, experimental points; lines, fits to the Stern−Volmer equation.

The kinetics of the quenching were used to study: (i) the ionic strength effect in the presence of potassium chloride at various concentrations, (ii) the anion effect and the Olson−Simonson effect in the presence of potassium salts of various anions with different charge types, such as KCl, KBr, KNO_3, K_2SO_4, and $K_3[Co(CN)]_6$, and (iii) the specific cation effects in the presence of 0.500 M cation solutions of MCl, M′Cl_2, or $R_nNH_{4-n}Cl$ (M = Li^+, Na^+, K^+, Cs^+, M′ = Mg^{2+}, Ca^{2+}, Sr^{2+}, Ba^{2+}; R = H, Me, Et, *n*-Pr; $n = 0-3$).

Within the experimental decay lifetime uncertainty of 0.1 μs, the hexacyanocobaltate ion, $[Co(CN)_6]^{3-}$ did not quench with any electrolyte. In contrast, for each of the acidopentacyanocobaltate complexes in solutions containing various alkali metal chlorides, efficient $[Pt_2(pop)_4]^{4-}$ quenching was observed and linear Stern-Volmer plots were obtained as shown for $[Co(CN)_5I]^{3-}$ and $[Co(CN)_5N_3]^{3-}$ in parts a and b of Figure 1, respectively. The derived second-order rate constants were found to range from 10^7 to 10^9 L mol^{-1} s^{-1}. The logarithmic values of the quenching rate constants in the presence of each cation at 0.500 M concentration are listed in Tables 2 and 3 and Table 1 in the Supporting Information. These constants decrease, Table 2, across the complex series $[Co(CN)_5I]^{3-}$ >

TABLE 2: $\log_{10} k_q$ for Quenching of $*[Pt_2(pop)_4]^{4-}$ by $[Co(CN)_5X]^{3-}$ (X = N_3, I, Br, Cl)[a]

	M				
X	Li^+	Na^+	K^+	NH_4^+	Cs^+
I	7.91 ± 0.01	8.10 ± 0.01	8.33 ± 0.03	8.35 ± 0.01	8.70 ± 0.01
N_3	7.73 ± 0.06	7.91 ± 0.03	8.10[b]	8.13 ± 0.04	8.46[b]
Br	7.39 ± 0.02	7.59 ± 0.01	8.02 ± 0.03	7.99 ± 0.02	8.41 ± 0.04
Cl	6.8 ± 0.2	7.12 ± 0.12	7.48 ± 0.05		7.84 ± 0.01

[a] Conditions: 0.010 M $HClO_4$/0.500 M MCl aqueous solutions at 22 °C. [b] Two coincident measurements. The rest are based on 3−5 measurements.

TABLE 3: log k_q for the Quenching of $*[Pt_2(pop)_4]^{4-}$ by $[Co(CN)_5I]^{3-}$ with Different Potassium-Containing Electrolytes[a]

electrolytes	$[K^+]$, M	μ, M	log k_q
KCl	0.50	0.51	8.33 ± 0.03
KBr	0.50	0.51	8.60 ± 0.01
KNO_3[b]	0.50	0.51	8.30 ± 0.02
K_2SO_4	0.50	0.76	8.28 ± 0.01
$K_3Co(CN)_6$	0.50	1.01	8.36 ± 0.01

[a] Conditions: 0.010 M $HClO_4$/0.50 M K^+ aqueous solutions at 22 °C. [b] KNO_3 itself quenches $*[Pt_2(pop)_4]^{4-}$, log k_q = 5.9 at 22 °C.

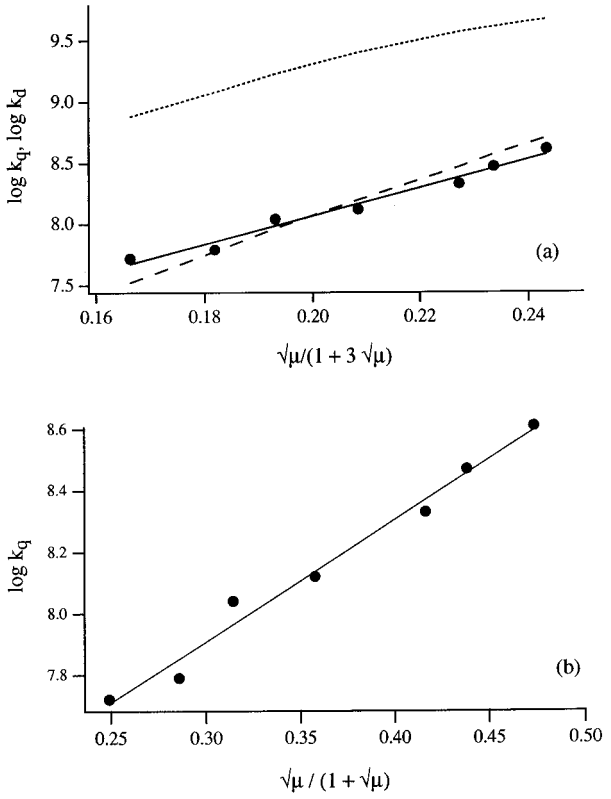

Figure 2. Dependence of $\log_{10} k_q$ on ionic strength in quenching of $*[Pt_2(pop)_4]^{4-}$ by $[Co(CN)_5I]^{3-}$ in KCl/0.010 M $HClO_4$ aqueous solution. Markers: experimental points. (a) Dotted line, $\log_{10} k_d$ calculated from eq 3; dashed line, fit to $\log_{10} k_q$ using eq 3 and 7 for k_d and k_{-d} with eq 2 for k_q and $k_t = 1.2 \times 10^9$ s^{-1}; solid line, fit to log k_q using eq 9. (b) Solid line, fit to $\log_{10} k_q$ using eq 10.

$[Co(CN)_5N_3]^{3-}$ > $[Co(CN)_5Br]^{3-}$ > $[Co(CN)_5Cl]^{3-}$ and also show a dependence on the nature of the cation.

The effect of ionic strength on the quenching rate constant was studied using $[Co(CN)_5I]^{3-}$ in KCl solutions with the results shown by the marker points in Figure 2 (numerical data with uncertainties are in Table 2 of the Supporting Information). Quenching efficiency increased with an increase in ionic strength, as would be expected for a collisional process involving two species having like charge.

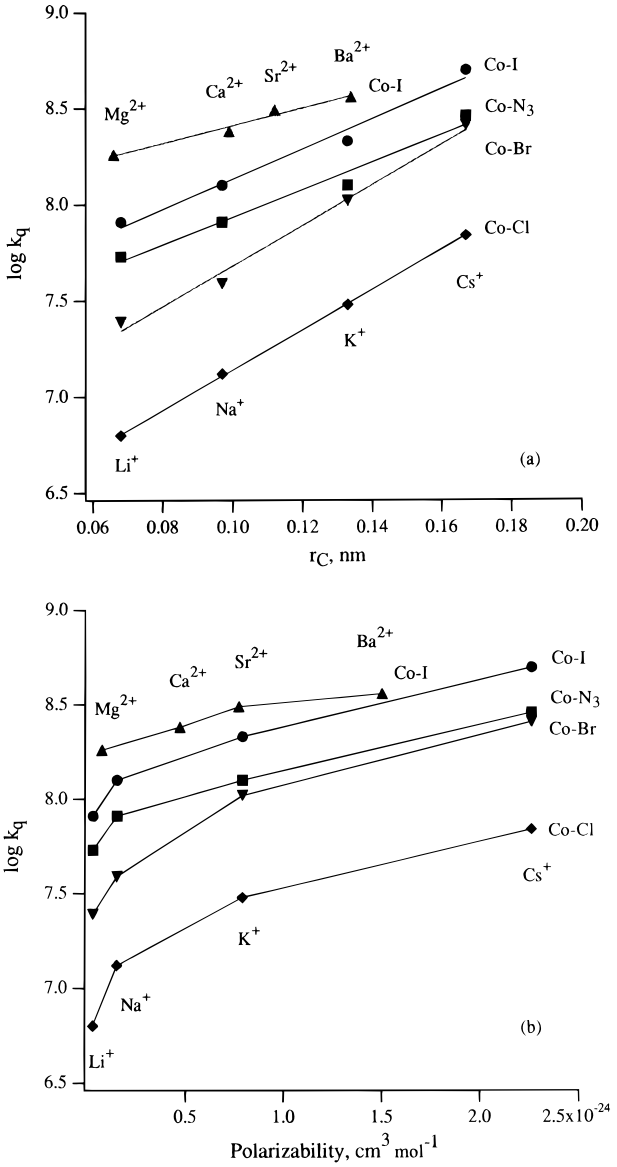

Figure 3. Specific cation effects on $\log_{10} k_q$ for the quenching of $*[Pt_2(pop)_4]^{4-}$ by $[Co(CN)_5I]^{3-}$. Conditions: 0.50 M cation/0.010 M $HClO_4$ solution. Markers, experimental points; lines, linear regression. (a) $\log_{10} k_q$ versus crystal radii; (b) $\log_{10} k_q$ versus polarizability.

The Olson−Simonson effect and the anion effect were tested at 0.5 M cation concentration by comparing the lifetime quenching in 0.50 M KNO_3 or KBr, 0.25 M K_2SO_4, and 0.167 M $K_3[Co(CN)]_6$ electrolytes. The derived logarithmic rate constants are shown in Table 3 and reveal that the quenching rate constant is linked to the concentration of cation and is independent of the nature of the anion except for bromide as discussed later.

Specific cation effects ranging over an order of magnitude were observed in the quenching rate constants such that Li^+ < Na^+ < K^+ < Cs^+, Table 2, and Mg^{2+} < Ca^{2+} < Sr^{2+} < Ba^{2+} (numerical values and uncertainties for this latter series are in Table 1 of the Supporting Information). For the series of alkali and alkaline earth metal cations, the logarithm of the rate constants was linear with the crystal radius[48] of the cation, r_C, Figure 3a, or the cation−water distance[49] (d_{M-O}), Figure 1a in the Supporting Information. Poor linear correlation was found, however, for log k_q vs the reciprocal of either the Stokes radius,[50] r_S, or the hydrated radius[50] of the cation, r_h, Supporting Information Figure 1b,c. Figure 3b shows that there was also a smooth nonlinear dependence on the polarizability (α) of the

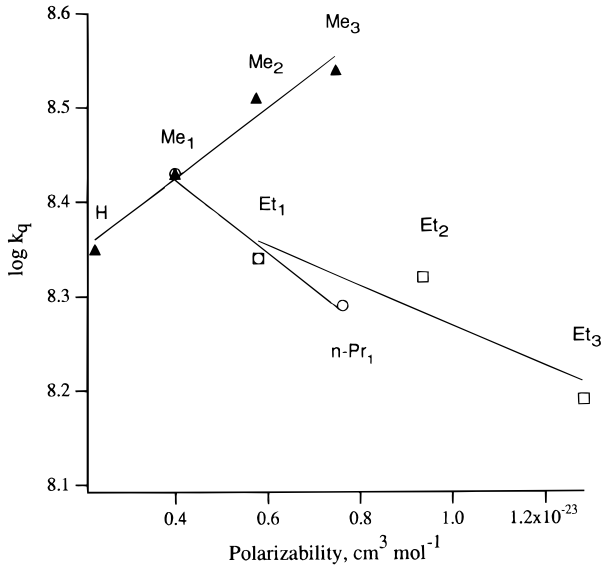

Figure 4. Specific cation effects on $\log_{10} k_q$ for the quenching of $*[Pt_2(pop)_4]^{4-}$ by $[Co(CN)_5I]^{3-}$. Conditions: 0.010 M $HClO_4$ / 0.50 M solutions of $R_nNH_{4-n}Cl$ (R = H, Me, Et, *n*-Pr; $n = 0-3$). Markers, experimental points; lines, linear regresssion.

cation,[51−53] consistent with the proportionality of polarizability with cation volume for simple spherical ions.

It is worth mentioning that only two sets of polarizability data for crystal alkaline or alkaline-earth metal ions were available,[51,53] and the values for a given ion differed as much as 40%. In contrast, the crystal cation radii,[48] r_C, and cation−water distances,[49] d_{M-O}, are more reliable. These gave good fits to the experimental data, as shown by the χ^2 value; for example, these range from 0.0002 to 0.0077 for the r_C fittings.

For the alkylammonium cations, $R_nNH_{4-n}^+$, the situation is more complex although all the effects seen were small, as shown in Figure 4. Here the data have been plotted versus polarizability as many of these ions are quite nonspherical and the measured polarizability is likely to be a relevant effective volume estimate. The quenching rate constants increased in the sequence $NH_4^+ < MeNH_3^+ < Me_2NH_2^+ < Me_3NH^+$, triangles in Figure 4. Contrasting trends occurred when the size of alkyl group increased from methyl to ethyl or *n*-propyl. The rate constants then decreased with increasing size and polarizability, $EtNH_3^+ > Et_2NH_2^+ > Et_3NH^+$, open squares, and $MeNH_3^+ > EtNH_3^+ > n\text{-}PrNH_3^+$, open circles in Figure 4.

Discussion

These results show that added electrolytes promote the quenching of triplet excited state $[Pt_2(pop)_4]^{4-}$ by the acidopentacyanocobaltate complexes. All four compounds quench to give small quantum yields of redox products, and the mechanistic details of these reactions are still under investigation using laser flash kinetic spectroscopy. We are still exploring the extent of atom/electron/energy transfer for the various complexes, but we have reported[25] that for the iodopentacyano system a novel iodine atom transfer from Co to Pt occurs. The quenching rate constant decreases by about an order of magnitude across the series $[Co(CN)_5I]^{3-} > [Co(CN)_5N_3]^{3-} > [Co(CN)_5Br]^{3-} > [Co(CN)_5Cl]^{3-}$, a feature which will be discussed[26] in the context of the reactivity studies. Here the discussion is focussed on the salt effects on the quenching rates.

Salt Effects. There are substantial salt effects on the quenching of $*[Pt_2(pop)_4]^{4-}$ by the acidopentacyanocobaltate complexes. For the anion $[Co(CN)_5I]^{3-}$, for example, the second-order rate constant increased by a factor of 7.8 from 5.2×10^7 to 4.1×10^8 M^{-1} s^{-1} as the concentration of KCl was increased from 0.1 to 0.8 M. First consider this effect in terms of the effect of electrolyte concentration on a reaction between charged species, assuming the usual kinetic mechanism for quenching between two species via diffusion-controlled formation of an encounter complex. That is, for dynamic quenching either by energy or electron transfer between excited state A and a quencher Q

$$A + Q \underset{k_{-d}}{\overset{k_d}{\rightleftharpoons}} \{A\cdots Q\} \xrightarrow{k_t} \text{Products} \qquad (1)$$

the overall bimolecular quenching rate constant is

$$k_q = k_d\left[\frac{k_t}{k_t + k_{-d}}\right] \qquad (2)$$

with k_d and k_{-d} dependent on salt concentration, conventionally via the ionic strength.

Exploration of the Ionic Strength Effect. The rate constants k_d and k_{-d} and the encounter pair equilibrium constant can be calculated using the Debye−Smoluchowski, Debye−Eigen, and Fuoss equations, respectively. We give these equations following Chiorboli et al.[1] but with the numerical constants appropriate for SI units. Thus

$$k_d = \frac{\dfrac{2000 k_B T N}{3\eta}\left[2 + \dfrac{r_A}{r_Q} + \dfrac{r_Q}{r_A}\right]}{a\displaystyle\int_a^\infty r^{-2} \exp\left[\frac{W(r,\mu)}{k_B T}\right] dr} \qquad (M^{-1}\ s^{-1}) \qquad (3)$$

where $W(r,\mu)$ is given according to Debye−Hückel theory by

$$W(r,\mu) = \frac{Z_A Z_Q e^2}{8\pi\epsilon^0 D} f(r,\mu) \qquad (J) \qquad (4)$$

where $f(r,\mu)$ and β are defined by

$$f(r,\mu) = \left[\frac{\exp(\beta\sigma_A\sqrt{\mu})}{1+\beta\sigma_A\sqrt{\mu}} + \frac{\exp(\beta\sigma_Q\sqrt{\mu})}{1+\beta\sigma_Q\sqrt{\mu}}\right]\frac{\exp(-\beta r\sqrt{\mu})}{r} \qquad (5)$$

$$\beta = \sqrt{\frac{8\pi N e^2 \rho_s}{4\pi\epsilon^0 D k_B T}} \qquad (mol^{-1}\,kg\,m^{-2})^{1/2} \qquad (6)$$

In these and the following equations, $k_B = 1.381 \times 10^{-23}$ J K^{-1}, $N = 6.022 \times 10^{23}$ mol^{-1}, $e = 1.602 \times 10^{-19}$ C, $\epsilon^0 = 8.854 \times 10^{-12}$ J^{-1} C^2 m^{-1}, T is the temperature, Z_A and Z_Q are the respective charges of the reactants, variable r represents the distance separating the two reactants, r_A and r_Q are the radii of the reactants, $a = r_A + r_Q$, σ_A (or σ_Q) is the sum radius (m) of reactant A (or Q) and the dominant counterion present, and μ is the ionic strength (mol kg^{-1}). For water at 298 K, $\rho_s = 997$ kg m^{-3}, $D = 78.54$, $\eta = 1.002 \times 10^{-3}$ N s m^{-2}.

The rate constant for the separation of encounter pairs, k_{-d}, can be determined from the Debye−Eigen equation:

$$k_{-d} = \frac{\dfrac{k_B T}{2\pi\eta a^2}\left[\dfrac{1}{r_A} + \dfrac{1}{r_Q}\right]\left[\dfrac{\exp[W(a,\mu)]}{k_B T}\right]}{a\displaystyle\int_a^\infty r^{-2} \exp\left[\frac{W(r,\mu)}{k_B T}\right] dr} \qquad (s^{-1}) \qquad (7)$$

The Fuoss equation for K_{eq} of the encounter pair is obtained from the ratio of eq 3 to eq 7:

$$K_{eq} = \frac{k_d}{k_{-d}} = \frac{4000\pi N a^3}{3} \exp\left[\frac{-W(a,\mu)}{k_B T}\right] \qquad (M^{-1}) \quad (8)$$

For our comparisons with theory, the diffusion-controlled rate constants k_d, k_{-d} and encounter pair equilibrium constant K_{eq} for the reactants $*[Pt_2(pop)_4]^{4-}$ and $[Co(CN)_5I]^{3-}$ in KCl/H^+ media were calculated at a temperaure of 295 K for various ionic strengths. To allow for the fact that $[Pt_2(pop)_4]^{4-}$ and $[Co(CN)_5I]^{3-}$ ions, particularly the former, are not truly spherical, their radii were estimated from $r = 0.5(d_x d_y d_z)^{1/3}$, where d_x, d_y, d_z are the dimensions measured along the three molecular axes of space-filling models generated by Chem-3D (CambridgeSoft), giving $r_A = r([Pt_2(pop)_4]^{4-}) = 0.43$ nm, $r_Q = r([Co(CN)_5I]^{3-}) = 0.47$ nm. The radius of the main counter ion was $r_{K^+} = 0.13$ nm. An obstacle to the general use of the above equations is the need to evaluate $f(r,\mu)$ over the appropriate range of r. Here the function was numerically integrated (Igor Pro 2.02 software, Wavemetrics) over the range of r from a to $30a$ in increments of $0.0145a$, which was checked to be an adequate range and increment to get the limiting value of the integral to less than 0.1% uncertainty.

The calculated values of log k_d are plotted as the dotted line in Figure 2a (numerical results are given in Supporting Information Table 3). The experimental quenching rate constants k_q are substantially lower than the calculated k_d values, $k_q < k_d$, Figure 2a, and quenching of $*[Pt_2(pop)_4]^{4-}$ by $[Co(CN)_5I]^{3-}$ belongs to the "nearly diffusion-controlled" regime because $k_t \approx k_{-d}$. A best fit of the experimental data for log k_q was obtained from eq 2 with $k_t = 1.2 \times 10^9$ s^{-1}, and the calculated values of k_d and k_{-d}, and is shown as the dashed line in Figure 2a. The satisfactory fit implies that the numerically integrated DE expressions give reasonable estimates of the diffusional parameters for ionic strength values as high as 0.8 M KCl in the systems studied here. Similar conclusions have been reached elsewhere[1,20,54] and they are particularly noteworthy as the Debye−Hückel theory makes several assumptions that are strictly valid only in very dilute solutions (<0.01 M), suggesting a fortunate cancellation of errors.

In the above, the calculated rate constant of the diffusive step k_d was obtained assuming pseudo-spherical reactants with a geometric average radius. This will be most adequate if all mutual orientations of the two reactants in the encounter complex correspond to the same reaction probability. In the system studied here, however, it is likely that the two reactants will need to approach each other in a special direction, such that the Co−X bond lines up with the open coordination site (z-axis) of $*[Pt_2(pop)_4]^{4-}$. Under this assumption, r_Q has the same value, but the value of r_A is reduced to 0.33 nm. This value leads to slightly smaller k_d and K_{eq} values, and larger k_{-d} and k_t values, but an equally good fit to the experimental results. Therefore the assumption of spherical reagents does not cause a major error.

A linear fit to the experimental rate constants can be obtained by using the Debye−Hückel−Brønsted (DHB) expression:

$$\log k = \log k^\circ + Z_A Z_Q \left[\frac{\sqrt{\mu}}{1 + \beta a \sqrt{\mu}}\right] \qquad (9)$$

The linear regression line that results, shown as the solid line in Figure 2a, has a slope of 11.6 ± 0.8, close to the charge product of the reactants, 12, and fits the data as well as, or even better than, the curve from the more rigorous expressions. This simplified equation is obtained by assuming equality of σ_A, σ_Q and a in eq 5, and for these reactants part of this assumption is very good since $r_A = 0.43 \approx r_Q = 0.47$, so that $\sigma_A = r_A + r_{K^+} \approx \sigma_Q$. Though these σ values are still quite a bit smaller than $a = r_A + r_Q$, the rate constant is not sensitive to small changes in either σ or a. For example, a decrease in the r_A value from 0.43 to 0.33 nm results in a slightly smaller slope of $Z_A Z_Q = 10 \pm 1$, still in reasonably good agreement with the charge product. The DHB model is therefore valid for rationalizing the relationship between the rate constant and ionic strength and gives the correct slope.

The familiar Debye−Brønsted limiting equation (DB)

$$\log k = \log k^\circ + Z_A Z_Q \left[\frac{\sqrt{\mu}}{1 + \sqrt{\mu}}\right] \qquad (10)$$

the expression often applied, leads to a reasonable linear fit of the data as shown in Figure 2b but fails to give a reasonable slope, the value being 4.0 ± 0.2. This is clearly because both reactants are large complex anions. The closest approach between these two reactants is 9 Å, much larger than the 3 Å typical of reaction between simple ions and required to obtain $\beta a = 1$ and give the DB equation. The calculations show the danger of using an oversimplified model when treating reaction between large coordination complexes.

The Olson−Simonson Effect. Unfortunately, the electrolytes which can be used for exploring the Olson−Simonson effect in this system are very limited in number. This is because many of the commonly used multivalent anions are either strong conjugate bases of weak acids (e.g. PO_4^{3-}, CO_3^{2-}, $C_2O_4^{2-}$) which will protonate in acidic media and change their charge type, are complexes which have strong absorptions at the excitation wavelength (e.g. $[Cr(CN)_6]^{3-}$), or are strong oxidizing or reducing agents such as $S_2O_8^{2-}$ and $S_2O_3^{2-}$ which will react[46] with excited state $*[Pt_2(pop)_4]^{4-}$. The results for the suitable electrolytes that were available nevertheless provided clear evidence that the Olson−Simonson effect operates in this system. For the quenching at pH = 2.0 of $*[Pt_2(pop)_4]^{4-}$ by $[Co(CN)_5I]^{3-}$, essentially the same quenching rate constant, log $k_q = 8.32$, was obtained in 0.167 M $K_3[Co(CN)_6]$, 0.25 M K_2SO_4, 0.500 M KCl, and 0.500 M KNO_3. These have a common K^+ concentration but an ionic strength that varies over a factor of 2, Table 3.

The Olson−Simonson effect has been observed for ground state reactions between anions and for one example of excited state electron transfer between cations. With the inclusion of the excited state reaction between anions of this work, it seems evident that the effect is rather general. Thus, in agreement with Chiorboli et al.[1] we conclude that when applying the Debye−Hückel equations to the reactions between species of like charge in the presence of electrolytes containing a multivalent ion, it is the concentration of the oppositely charged ion(s) rather than the ionic strength that should be used. Taken together with the observation that the interaction between $*[Pt_2(pop)_4]^{4-}$ and $[Co(CN)_5X]^{3-}$ is unobservable in the absence of added cations but is strongly promoted in their presence, this leads us to conclude that the cation may play an important role in the transition state of the reaction rather than just serving as an "inert" or "supporting" electrolyte. This is discussed in more detail below and is likely the reason for the observation of the Olson−Simonson effect rather than the general ionic strength effect.

Anion Effects. As shown in Table 3, there is no effect of the anion when multivalent oxyanions or a complex anion is used. The nucleophilic bromide anion showed a special effect, however. Table 3 shows that the logarithmic quenching rate constant was 8.60 in 0.50 M KBr, larger than the value of 8.33 in 0.50 M KCl. This effect seems explicable in terms of an influence of anion nucleophilicity on the rate constant k_t, as

will be discussed in the paper[25] on the electron transfer and atom transfer processes found for these systems.

Specific Cation Effects. Extensive studies were made of the cation effect on the quenching rate constant, and Figure 3 shows that for alkali metal or alkaline-earth cations, the quenching rate constants increase with cation crystallographic radius or polarizability. Any attempt to use the Debye−Eigen equation to explain these cation effects in terms of changes in k_d will fail; varying the cation radius used in the calculation of diffusion-controlled rate constants has only a very small effect, negligible in comparision to the observed specific cation effects. For example, k_d for the reaction between $*[Pt_2(pop)_4]^{4-}$ and $[Co(CN)_5I]^{3-}$ should *decrease* about 8% with an increase in cation radius from Li^+ to Cs^+, completely contradicting the experimental results, which show a 6-fold *increase*. A similar phenomenon was reported[1,55] earlier.

This comparison invites a consideration of the possible effects of flaws in the Debye−Smoluchowski−Eigen treatment. It assumes that the solvent is unstructured and isotropic, and only considers purely electrostatic interactions between charged species, neglecting all other interactions including solvent−substrate interactions.[55] This is undoubtedly a problem in aqueous solutions due to the variations of the solvent structure with electrolyte addition and the presence of other interactions, such as H-bonding.

It is known that the addition of certain electrolytes causes water molecules in the solution to become more or less structured compared to pure water.[56] In the presence of alkali and alkaline-earth cations, the water molecules in the immediate vicinity of the ion are oriented and partially immobilized by electrostatic attraction to the cation leading to a shell with increased water structure. The extent of this effect depends on the charge density of the ion and is therefore inverse with the "bare" ionic radius, i.e. the structure-making ability of $Li^+ > Na^+ > K^+ > Cs^+$ and $Mg^{2+} > Ca^{2+} > Sr^{2+} > Ba^{2+}$. In a more structured aqueous solution, the mobility of the reactant ions is likely to be lowered, decreasing the diffusion rate constant (k_d) and hence the quenching rate constant. This prediction is in the correct direction to agree with our experimental results. However, the increase in quenching rate constant from Li^+ to Cs^+ (a factor of 6−11 for different acidopentacyanocobaltates) is much too large to reasonably attribute to these effects. It is therefore inadequate to use these arguments alone to try explain the specific cation effects.

This leads us to consider the likelihood of a more intimate involvement of the cation in the transition state for the quenching process which would influence the overall rate constant by its effect on the rate constant for electron/atom/energy transfer, k_t. Such involvement is supported by the observation of the Olson−Simonson effect. The cation will be located between the anionic reagents because of its earlier role to help overcome the significant Coulombic barrier associated with formation of the encounter pair. Also extensive desolvation may be expected on interaction of the cation with the strongly anionic reactants. As evidence of this in analogous systems, positive activation volumes $\Delta V^{\ddagger}$ have been reported for the $[Fe(CN)_6]^{4-}/[Fe(CN)_6]^{3-}$ self-exchange catalyzed by potassium ion[57] and the electron transfer reaction between $*[(Mo_6Cl_6)Cl_6]^{2-}$ and $[IrCl_6]^{2-}$ in a solution containing Na^+ cation.[21] The idea of transition state participation by a desolvated cation which can act as a conduit for electron/energy transfer is consistent both with the linear correlations observed between the quenching rate constant and the cation crystal radius, Figure 3a, and with the poor correlations between log k_q and the reciprocal of the hydrated radii and Stokes radii, Supporting Information Figure 1b,c (the latter contrasting with the conclusions[21,22] of some other work). There is also a smooth trend with cation polarizability, Figure 3b, but these plots are nonlinear; this nonlinearity is consistent with the theoretical relationship of polarizability to the cube of the cation radius. Indeed plots of these logarithmic rate constants versus the cube root of the polarizability also give good straight lines.

Table 2 and Figure 3a,b show that the cation effect is in the same direction for all four quenchers, $[Co(CN)_5Br]^{3-}$, $[Co(CN)_5Cl]^{3-}$, $[Co(CN)_5I]^{3-}$, and $[Co(CN)_5N_3]^{3-}$. However they fall roughly into two groups on the basis of their sensitivities to the size of the cation. The quenching rate constant increased about 10−11 times from Li^+ to Cs^+ in the first group (i.e. $[Co(CN)_5Br]^{3-}$ and $[Co(CN)_5Cl]^{3-}$), but only 5−6 times in the second group (i.e. $[Co(CN)_5I]^{3-}$ and $[Co(CN)_5N_3]^{3-}$). These results imply that the nature of the cation involvement in the transition state varies for the different quenchers. The cation can assist quenching by forming either a linear or triangular ion triplet with the reactants, both of which configurations have been proposed[15] for other systems. Of the two, the linear arrangement is likely to show greater sensitivity of the quenching rate constant to the size of the cation. Application of these ideas to our systems suggests that in the X = Br, Cl group the cation may be in the center of a linear transition state, while in the X = I, N_3 group the nonlinear ion triplet is more important. We are trying to explore this supposition further by exploring its possible influence on the extent of atom and electron transfer reaction.[26]

In an effort to quantify such specific cation effects on reactions, Pethybridge introduced, measured, and tabulated[58] specific interaction coefficients $B_{i,j}$ for the interaction between oppositely charged ions i and j by defining the activity coefficient of an ion f_i in the presence of oppositely charged ions by

$$-\log f_i = AZ_i F(\mu) - \sum_j B_{i,j} C_j \qquad (11)$$

where $F(\mu)$ is some function of the ionic strength. The coefficient $B_{i,j}$ will be negative or positive depending on whether there are attractive or repulsive interactions (not including the Coulomb attraction) between the ions at close range. Two opposing trends (α and β) of specific interaction coefficients were found for various reactant anions interacting with alkali metal, alkaline-earth metal, and tetraalkylammonium salts. For anions of high charge density, such as OH^-, F^-, and acetate, $B_{i,j}$ interaction coefficients become increasingly positive with the increasing size of "bare" cation, an α (or growth) sequence, while anions with a well-dispersed charge show the opposite, β (or decline), trend. Unfortunately such coefficients are not available for our reactant ions, so these ideas cannot be applied quantitatively to our results. The best that can be achieved is a rationale based on recognizing that the quenching rate constant is predicted to vary as

$$\log k_q = \log k^\circ + 2AF(\mu) + \{B(*[Pt_2(pop)_4]^{4-}) + B([Co(CN)_5I]^{3-}) - B(\text{ion triplet})\}[C_{\text{cation}}] \qquad (12)$$

Both reactants are large anions with B coefficients that should show a β trend. The postulated ion triplet transition state will be larger and have a better distributed charge, so $B_{\text{ion triplet}}$ should show an even stronger β sequence. To explain our net overall α trend then requires that this last term dominate so that, combining the three trends, $\beta(*[Pt_2(pop)_4]^{4-}) + \beta([Co(CN)_5I]^{3-}) -$ large β(ion triplet) $\approx \alpha$(overall). In summary, this type of analysis supports our conclusion that the specific ion effects

observed have their origin in effects on an ion triplet transition state for reaction.

The effects of the alkylammonium cations on the rate constants are somewhat different than those of the simple inorganic cations discussed above. The effects are quite large, with ammonium ion being slightly more effective than potassium ion, but the variations between different alkylammoniums are quite small. Figure 4, triangles, shows that the quenching rate constants for the methylammonium cations increase by an overall 50% with increasing number of methyl groups and correlate with the polarizability. Earlier studies have shown that these methylammonium cations mimic large simple inorganic cations analogous to Cs^+, so that any effects on the rate constant k_d could be explained in terms of their electrostrictive structure making. Across the series, the increasing size with number of methyl groups results in a decrease in charge density of the cation and fewer structured water molecules, so a small increase in the k_d contribution to the quenching rate constant may be expected, $NH_4^+ < MeNH_3^+ < Me_2NH_2^+ < Me_3NH^+$.

For the series with increasing number of ethyl groups, $EtNH_3^+ \geq Et_2NH_2^+ \geq Et_3NH^+$, open squares in Figure 4, the quenching rate constant does not change; this is due to the small structure-making effects of ethylammonium ions which have been attributed[59,60] to opposing trends in the electrostatic and hydrophobic contributions to water structuring. These electrolytes are therefore a good choice to study quenching interactions between charged species without the complication of variations in specific ion effects on k_d.

For alkylammoniums with larger alkyl groups, open circles in Figure 4, the effect on water structure is different. The finding that k_q for $MeNH_3^+ > EtNH_3^+ > n\text{-}PrNH_3^+$ is consistent with the increasing water structure associated with the larger alkyl groups; this arises[7,9,56,61,62] because the water is required to form a structured cavity to accommodate them.

Since the quenching rate constant variations with different alkylammonium salts are relatively small (a factor of only 1.5 overall) and can be reasonably associated with changes in water structure, we conclude that these ions are involved in the transition state in a way that does not lead to large variations in k_t across the series. This may be, as a referee has suggested, because the positive charge center is similar in all these ions and therefore contributes to k_t with roughly constant efficiency across the series.

Conclusions

For the quenching interaction between anionic species studied here, the effect of univalent electrolyte concentration on the rate constants is well accounted for by the Debye−Smoluchowski−Eigen equations, and even by the Debye−Hückel−Bronsted equation, up to much higher concentrations than would be expected theoretically. When multiply charged ions are present, however, the ionic strength should be replaced by the concentration of the counterion of opposite charge. For alkali and alkaline-earth cations, linear correlations of the logarithmic rate constant with bare ion radius or polarizability were seen and across the series of ions studied, large specific ion effects were observed, indicating that these ions intimately participate in the transition state for the interaction. In contrast, alkylammonium ions showed small variations of logarithmic rate constant with polarizability, and these variations were qualitatively as would be expected from their known effects on water structure and hence on the diffusion coefficients for the reactant anions.

Acknowledgment. The authors thank the X-ray powder photography service of the University of Bern for the X-ray data. Financial support was provided by the Natural Sciences and Engineering Research Council of Canada and the University of Victoria.

Supporting Information Available: Tables giving effects of cation, concentration, and ionic strength on log k_q; figures showing log k_q versus cation−water distance and reciprocals of the Stokes radii and hydrated radii (5 pages). Ordering information is given on any current masthead page.

References and Notes

(1) Chiorboli, C.; Indelli, M. T.; Scandola, M. A. R.; Scandola, F. *J. Phys. Chem.* **1988**, *92*, 156.
(2) Olson, A. R.; Simonson, T. R. *J. Chem. Phys.* **1949**, *17*, 1167.
(3) Ferranti, F.; Indelli, A. *J. Chem. Soc., Faraday Trans. 1* **1989**, *85*, 2241.
(4) Ferranti, F. *J. Chem. Soc. A* **1970**, 134.
(5) Kershaw, M. R.; Prue, J. E. *Trans. Faraday Soc.* **1967**, *63*, 1198.
(6) Basu, M. K.; Das, M. N. *J. Chem. Soc. A* **1968**, 2182.
(7) Zamboni, R.; Giacomelli, A.; Malatesta, F.; Indelli, A. *J. Phys. Chem.* **1976**, *80*, 1418.
(8) Indelli, A.; Nolan, G.; Amis, E. S. *J. Am. Chem. Soc.* **1960**, *82*, 3237.
(9) Campion, R. J.; Deck, C. F.; King, P.; Wahl, A. C. *Inorg. Chem.* **1967**, *6*, 672.
(10) Fava, A.; Bresadola, S. *J. Am. Chem. Soc.* **1955**, *77*, 5792.
(11) Scandola, M. A. R.; Scandola, F.; Indelli, A. *J. Chem. Soc., Faraday Trans. 1* **1985**, *81*, 2967.
(12) Braga, T. G.; Wahl, A. C. *J. Phys. Chem.* **1985**, *89*, 5822.
(13) Stalnaker, N. D.; Solenberger, J. C.; Wahl, A. C. *J. Phys. Chem.* **1977**, *81*, 601.
(14) Basolo, F.; Pearson, R. G. Oxidation-Reduction Reactions. *Mechanisms of Inorganic Reactions*; John Wiley and Sons, Inc.; New York, 1967.
(15) Shporer, M.; Ron, G.; Loewenstein, A.; Navon, G. *Inorg. Chem.* **1965**, *4*, 361.
(16) Spiccia, L.; Swaddle, T. W. *Inorg. Chem.* **1987**, *26*, 2265.
(17) Rasmussen, P. G.; Brubaker, C. H. *Inorg. Chem.* **1964**, *3*, 977.
(18) Leipoldt, J. G.; Bok, L. D. C.; Wyk, A. J. V.; Dennis, C. R. *J. Inorg. Nucl. Chem.* **1977**, *39*, 2019.
(19) Gaines, G. L. *J. Phys. Chem.* **1979**, *83*, 3088.
(20) Greiner, G.; Pasquini, P.; Weiland, R.; Orthwein, H.; Rau, H. *J. Photochem. Photobiol. A* **1990**, *51*, 179.
(21) Tanaka, H. K.; Sasaki, Y.; Saito, K. *Inorg. Chim. Acta* **1993**, *210*, 63.
(22) Yamaguchi, T.; Sasaki, Y. *Inorg. Chem.* **1990**, *29*, 493.
(23) Kirk, A. D.; Kneeland, D. M. *Inorg. Chem.* **1995**, *34*, 1536.
(24) Kneeland, D. M. The Photochemistry of $[Co(CN)_5X]^{3-}$ Complexes. Doctoral Dissertation, 1991.
(25) Kirk, A. D.; Cai, L. *Chem. Commun.* **1997**, 523.
(26) Cai, L.; Kirk, A. D. To be published.
(27) Gmelin. Azidosalze $[CoN_3A_5]X_2$. *Gmelins Handbuch Der Anorganischen Chemie*; Verlag Chemie Gmbh: Weinheim-Bergstr, 1964.
(28) Fujita, J.; Shimura, Y. *Bull. Chem. Soc. Jpn.* **1963**, *36*, 1281.
(29) Abou-El-Wafa, M. H. M.; Burnett, M. G.; McCullagh, J. F. *J. Chem. Soc., Dalton Trans.* **1986**, 2083.
(30) Flor, T.; Casabo, J. *Synth. React. Inorg. Met.-Org. Chem.* **1986**, *16*, 795.
(31) Haim, A.; Wilmarth, W. K. *J. Am. Chem. Soc.* **1961**, *83*, 509.
(32) Grassi, R.; Haim, A.; Wilmarth, W. K. *Inorg. Chem.* **1967**, *6*, 237.
(33) Miskowski, V. M.; Gray, H. B. *Inorg. Chem.* **1975**, *14*, 401.
(34) Wrighton, M.; Bredesen, D.; Hammond, G. S.; Gray, H. B. *J. Chem. Soc., Chem. Commun.* **1972**, 1018.
(35) Gutterman, D. F.; Gray, H. B. *J. Am. Chem. Soc.* **1971**, *93*, 3364.
(36) Alexander, K. A.; Bryan, S. A.; Dickson, M. K.; Hedden, D.; Roundhill, D. M.; Che, C.-M.; Butler, L. G.; Gray, H. B. *Inorg. Synth.* **1986**, *24*, 211.
(37) Zipp, A. P. *Coord. Chem. Rev.* **1988**, *84*, 47.
(38) Che, C.-M.; Butler, L. G.; Gray, H. B. *J. Am. Chem. Soc.* **1981**, *103*, 7796.
(39) Fordyce, W. A.; Brummer, J. G.; Crosby, G. A. *J. Am. Chem. Soc.* **1981**, *103*, 7061.
(40) Shimizu, Y.; Tanaka, Y.; Azumi, T. *J. Phys. Chem.* **1984**, *88*, 2423.
(41) Rice, S. F.; Gray, H. B. *J. Am. Chem. Soc.* **1983**, *105*, 4571.
(42) Murov, S. L.; Carmichael, I.; Hug, G. L. *Handbook of Photochemistry*; Marcel Dekker, Inc.: New York, Basel, Hong Kong, 1993.
(43) Demas, J. N. *Excited State Lifetime Measurements*; Academic Press: New York, 1983.
(44) Fetterolf, M.; Friedman, A. E.; Yang, Y.-Y.; Offen, H.; Ford, P. C. *J. Phys. Chem.* **1988**, *92*, 3760.
(45) Roundhill, D. M.; Gray, H. B.; Che, C.-M. *Acc. Chem. Res.* **1989**, *22*, 55.

(46) Peterson, J. R.; Kalyanasundaram, K. *J. Phys. Chem.* **1985**, *89*, 2486.
(47) Kalsbeck, W. A.; Gingell, D. M.; Malinsky, J. E.; Thorp, H. H. *Inorg. Chem.* **1994**, *33*, 3313.
(48) Weast, R. C.; Lide, D. R.; Astle, M. J.; Beyer, W. H. *CRC Handbook of Chemistry and Physics*; CRC Press Inc.: Boca Raton, FL, 1990.
(49) Marcus, Y. *Chem. Rev.* **1988**, *88*, 1475.
(50) Nightingale, E. R. *J. Phys. Chem.* **1959**, *63*, 1381.
(51) Rao, C. N. R.; George, M. V.; Mahanty, J.; Narsimhan, P. T. *A Handbook of Chemistry and Physics*; Van Nostrand Reinhold Company: London, 1970.
(52) Rosseinsky, D. R. *J. Am. Chem. Soc.* **1994**, *116*, 1063.
(53) Fowler, P. W.; Pyper, N. C. *Proc. R. Soc. London A* **1985**, 377.
(54) Chiorboli, C.; Scandola, F.; Kisch, H. *J. Phys. Chem.* **1986**, *90*, 2211.
(55) Rexwinkel, R. B.; Meskers, S. C. J.; Dekkers, H. P. J. M.; Riehl, J. P. *J. Phys. Chem.* **1992**, *96*, 5725.
(56) Frank, H. S.; Wen, W.-Y. *Discuss. Faraday Soc.* **1957**, *24*, 133.
(57) Tagaki, H.; Swaddle, T. W. *Inorg. Chem.* **1992**, *31*, 4669.
(58) Pethybridge, A. D.; Prue, J. E. *Prog. Inorg. Chem.* **1972**, *17*, 327.
(59) Blandamer, M. J. *Q. Rev., Chem. Soc.* **1970**, *24*, 169.
(60) Sarma, T. S.; Ahluwalia, J. C. *Chem. Soc. Rev.* **1973**, *2*, 203.
(61) Ashford, N. F.; Blandamer, M. J.; Burgess, J.; Laycock, D.; Waters, M.; Wellings, P.; Woodhead, R.; Mekhail, F. M. *J. Chem. Soc., Dalton Trans.* **1979**, 869.
(62) Millero, F. J. The Partial Molal Volumes of Electrolytes in Aqueous Solutions. *Water and Aqueous Solutions*; Wiley: New York, 1972.